Vol. 29, No. 2, 2025, Pages 118-132

Thi-Qar Medical Journal (TQMJ)

Thi-Qar Medical Journal was established in 2006 and is published by the College of Medicine, University of Thi-Qar, Iraq

ISSN (PRINT): 1992-9218 | ISSN (ONLINE): 3006-4791

www.jmed.utq.edu.iq utjmed@utq.edu.iq

Portable Microfluidic Devices-Based Nanosensors for Detection of Mercury and Cadmium in Blood Plasma

Baheya Abdulbaqi Alaziz [1], Mundher Al-Shakban *[2], Zaidon T. Al-aqbi *[3]

[1] Department of Physics, College of Science, University of Misan, Maysan, 62001 Iraq.

[2] Department of Chemistry, College of Science, University of Misan, Maysan, 62001, Iraq.

Correspondence; Mundher.Al-Shakban@uomisan.edu.iq.

Received:4-7-2025
Revised:12-8-2025
Accepted: 30-9-2025
DOI:
10.32792/jmed.2025.29.32

Keywords:
Heavy metals
Microfluidics
Nano structure
Hg^{2+} detection
Cd^{2+} detection.

How to cite

Baheya Abdulbaqi Alaziz [1], Mundher Al-Shakban [2], Zaidon T. Al-aqbi [3]. Portable Microfluidic Devices-Based Nanosensors for Detection of Mercury and Cadmium in Blood Plasma. *Thi-Qar Medical Journal (TQMJ)*.2025;Volume(29):118-132.

Heavy metals such as cadmium (Cd^{2+}), mercury (Hg^{2+}), and lead (Pb^{2+}) are considered some of the most dangerous environmental pollutants due to their high toxicity and cumulative effects on human health and the environment. With the increasing need for precise, rapid, and highly sensitive detection technologies, the integration of nanomaterials with microfluidic techniques has emerged as one of the effective solutions in developing advanced sensing systems Nanomaterials provide unique properties such as high surface area and distinctive electrochemical and optical characteristics, enabling them to capture heavy metal ions with exceptional efficiency. When integrated into microfluidic platforms (Lab-on-a-Chip), a precise analytical environment is achieved, enabling detection using minimal amounts of samples and reagents, with a short analysis time.
These systems are characterized by their ability for on-site detection. Various characterization measurements such as UV, XRD, FESEM, TEM, FT-IR, and Zeta Potential were conducted to characterize the nanoparticles. The study indicated that the best elements used for detecting heavy metals in blood plasma are zinc oxide and copper. This integration is considered one of the promising recent trends in the field of environmental monitoring and precise medical analysis.

Copyright: ©2025 The authors. This article is published by the Thi-Qar Medical Journal and is licensed under the CC BY 4.0 license

1. Introduction

Heavy metals are a group of elements with high atomic weights and densities that can be toxic even at low concentrations. In human blood, heavy metals include both essential trace elements necessary for physiological function and toxic elements that pose

significant health risks when accumulated beyond safe thresholds. Monitoring heavy metal concentrations in blood is crucial for assessing environmental and occupational exposures, diagnosing poisoning, and preventing long-term health effects [1,2].

Measuring heavy metal concentrations in blood is a standard biomonitoring practice used to assess individual and population exposure, guide clinical interventions, and inform regulatory standards. Advanced analytical techniques, including atomic absorption spectroscopy (AAS), inductively coupled plasma mass spectrometry (ICP-MS), and emerging nanomaterial-based sensors, offer precise quantification at trace levels, supporting early detection and prevention of toxic metal exposure [3] Many researchers have found various means to detect this type of ions. For instance, the researcher Le Ma, Wen-Yuan Pei prepared a new and practical magnetic nanomaterial with a core-shell structure, Fe @Ag@dimercaptobenzene (Fe @Ag@DMB), using sodium borohydride as a reducing agent in a one-step method. His study demonstrated that the functional thiol groups on the newly synthesized magnetic nanoparticles can interact with Cd^{2+}, Pb^{2+}, and Hg^{2+} ions in water samples, thus achieving effective extraction of Cd^{2+}, Pb^{2+}, and Hg^{2+}.ions [4].
For the sensitive and stable detection of airborne heavy metals. By optimizing the balance between thread length and detection distance, the FIFS system achieved its best performance, with a limit of detection (LOD) for lead in heavy metals at 0.3 picograms /m^3 and a minimum detectable concentration of 0.47 picograms/m^3 at a distance of 10 meters. The relative standard deviation (RSD) remained below 7% across a wide range of concentrations, indicating the high stability of the system. In addition to lead (Pb), the system also succeeded in detecting airborne cadmium (Cd), mercury (Hg), and cobalt (Co), all within measurable detection limits[5]. Nanomaterials such as zinc oxide (ZnO), nickel oxide (NiO), and cobalt oxide (Co_3O_4) have shown exceptional potential in sensing applications due to their tunable surface properties, high surface area, and ability to facilitate electron transfer reactions. These metal oxide nanoparticles can be functionalized with specific chelating agents or ligands to enhance the selective binding of Cd^{2+} and Hg^{2+} ions. When used as modifiers on electrode surfaces, hey improve signal response, reduce background noise, and enhance the sensitivity of electrochemical detection systems [6, 7].

Despite the success of most heavy metal detection methods, the search for faster and more sensitive methods continues due to the increasing necessity of detecting this type of element.

Nanomaterials have unique properties such as high chemical reactivity, large surface area, and the ability to undergo surface modification, making them suitable for use in various fields [8,9], Alexandra Pricop and other researcher prepared copper nanoparticles using the chemical reduction method and obtained spherical nanoparticles through this method. He indicated in his study the possibility of using them in therapeutic applications (cancer treatment) after studying the potential cellular toxicity that depends on the dose. The resulting spherical copper nanoparticles were also used in industrial fields such as 2D and 3D printing [10, 11]

Many researchers have also attended the zinc nanoparticles, as these particles have proven successful in various fields, including Antioxidant, anticancer, drug delivery Sensors, electronic devices[12,13,14].

Microfluidics are small devices that process fluids within very fine channels and play increasingly important roles in the field of biomedicine due to their high detection efficiency [15]. Liu et al. studied the development of microfluidic valves for the management of biological fluids and time-sampling, in addition to active triggers in feedback control [16], other researchers also studied the use of precise liquid devices based on multi-colored paper for rapid on-site testing of bacteria causing diseases in water and food products [17].

In this research paper, we designed and manufactured a new microfluidic device with a very small size, printed using 3D printing technology for localized detection. We use nanomaterials prepared by the green synthesis method, such as zinc oxide and copper, to detect mercury and cadmium ions at the lowest concentrations found in blood plasma .Detection is carried out thru the color change that occurs during the detection process.

1.1. Methodology and Approaches

Material

The Boswellia sacra grains purchased from Basra Governorate, Iraq, and were ground and extracted in the laboratories of Maysan University, College of Science. Sodium hydroxide (NaOH), hydrazine hydrate $N_2H_5.H_2O$, copper sulfate ($Cu\ SO_4\ .5H_2O$) and Cadmium Sulfate ($CdSO_4$) were purchased from LOBA Chemi in Rajasthan, India. Zinc Acetate Zn $(CH_3CO_2)_2(H_2O)$ purchased from Fengcheng in Chaina. Mercuric Chloride ($HgCl_2$) purchased from Thomas Baker in India.

Methods

Preparation of the Boswell sacra (BS) Extract Solution

The Boswell sacra extract solution of 1% was prepared using a method by Al-aqbi et al. [18]. Firstly, the Boswella sacra solid particles were crushed by a mill to get a fine powder. Then, 1 g of the Boswell sacra powder was moved to a conical flask and left dissolving and stirring with 100 mL of distilled water for 30 min at 70 °C. Finally, the mixture was filtered by centrifuge machine at a speed of 500 rpm for two minutes each time using plastic containers with a capacity of 15 ml and stored in a refrigerator at 5 °C to be used for in the synthesis of nano particles.

Green synthesis of copper nanoparticles

The copper nanoparticles were prepared by adding 5 ml of (0.1 M) copper sulfate ,8 ml of (0.01 M) NaOH, and 8 ml of 1% BS were combined in a capped glass bottle and for 5 minutes, the mixture was heated to 75 °C and stirred at a speed of 500. After that, 3 ml of 88% N_2H_5OH (hydrazine) was added to the reactor solution gradually, and it was continuously stirred until the pH reached 10 after 30 minutes. When hydrazine was added, the color gradually changed from light blue to blue to green to yellow until it reached dark red. Then the solution is filtered by a centrifuge machine at a speed of 500 RPM for 2 minutes each time using plastic containers with a capacity of 15 ml. The material was collected, distilled water was added to it, and it was placed again in the centrifuge. The separation process was repeated 3 times, and then the result was placed in a Petri dish covered with perforated foil at laboratory temperature for two days until it dried. Then the material was collected, and it was in the form of a reddish-brown powder.

Green synthesis of Zinc oxide nanoparticles

Zinc oxide nanoparticles were prepared using the method [18], in the preparation of copper nanoparticles with some modifications. 5 ml of 0.1 M and 8 ml of 0.1 NaOH were added, then 8 ml of 1% BS extract were added, where the solution gradually changed from transparent to white. After 5 minutes, 3 ml of 88% N_2H_5OH (hydrazine) was added, and white precipitates began to appear, making the solution whiter. The reaction continued for 45 minutes at a temperature of 70°C and was stirred at a speed of 350. Then the solution is filtered by a centrifuge machine at a speed of 500 RPM for 2 minutes each time using plastic containers with a capacity of 15 ml. The material was collected, distilled water was added to it, and it was placed again in the centrifuge. The separation process was repeated three times, and then the result was placed in a Petri dish covered with perforated foil at laboratory temperature for 24 hours until it dried. Then the material was collected, and it was in the form of a white powder.

Preparation of (cadmium and mercury) Solution

To obtain (0.1m M) cadmium, dissolve 0.00104 g from cadmium sulfate in 50 ml of distilled water at a temperature of 50 °C and a speed of 500 RPM for 18 minutes and to obtain a 0.1 molar solution of mercury, dissolve 0.000368 g of mercuric chloride in 50 ml of distilled water at a temperature of 50 °C and a speed of 500 RPM for 10 minutes.

Preparing blood plasma sample .

The traditional rapid method involves using a 15 ml special glass tube containing anticoagulants to prevent blood clotting. The drawn blood sample is placed in the tube. It is left for 10-15 minutes, then the tube is gently inverted three times and placed in a centrifuge for 10 min at 5000 RPM. After the separation process is complete, the plasma is carefully drawn using a plastic pipette and stored in a 10 ml test tube at a temperature of 5 °C until use.

Detection of Cadmium by ZnO NPs

Cadmium is considered a heavy metal, and if its concentration exceeds 5 micrograms/liter, it becomes toxic according to the American Conference of Governmental and Industrial Hygienists[19].To detect the presence of the lowest concentration of it

in blood plasma, we take the concentrations (0.5, 1, 1.5, 2, 2.5) mg/L using a pipette and place each in a 5 mL test tube. We add 0.2 mL of the Zinc oxide nanoparticle filtrate diluted with distilled water to 2 m L. When measuring the absorbance with a UV device for each concentration, a difference in absorbance was observed with the addition of the reagent and before the addition. Therefore, 25 mg/L of the previously prepared blood plasma is taken, and the lowest concentration of Cadmium substance, 0.5 mg/L, is added to it, along with 2 mL of the diluted zinc Oxide nanoparticle filtrate.

Detection of mercury by Cu NPs

Mercury is one of the toxic elements, and exceeding the normal levels in the blood leads to numerous health risks for humans. To detect the presence of the lowest concentration of it in blood plasma, we take the concentrations (0.5, 1, 1.5, 2, 2.5) mg/L using a pipette and place each in a 5 mL test tube. We add 0.2 mL of the Copper nanoparticle filtrate diluted with distilled water to 2 mL. When measuring the absorbance with a UV device for each concentration, a difference in absorbance was observed with the addition of the reagent and before the addition. Therefore, 25 mg/L of the previously prepared blood plasma is taken, and the lowest concentration of Cadmium substance, 0.5 mg/L, is added to it, along with 2 mL of the diluted Copper nanoparticle filtrate.

Microfluidic device

The microfluidic device was drawn and designed using the SolidWorks 2022 design software and then printed using the Object Eden 260VS 3D printer, resulting in a 3D model with dual device with two channels (30 x 13 × 10) [20] as shown in (figure 1)To prepare the microfluidic device for use, we soak the device in distilled water for 2 hours, then place it in an ultrasonic device for 10 minutes at 92% power and 40 kHz frequency. Finally, it is placed in a 0.1M sodium hydroxide solution for 40 minutes, washed with water, and left to dry completely to be ready for use.

1.2. Results and Conclusions

UV-Vis spectroscopic studies are the primary option for confirming the presence of most nanoparticles [21], as they provide a quick and accurate method for understanding the physical and chemical properties of materials. It is considered one of the essential analytical tools widely used in various scientific fields (research paper), where figure 2 illustrates the UV spectrum of ZnO. The visible UV spectrum of green-synthesized zinc oxide nanoparticles is observed in the figure. The maximum absorption peak appears at 369.5 nanometers as shown in curve A. It was mentioned in [22] that the clear peak of zinc oxide disappears upon the addition of the toxic element Cd solution, as indicated by the straight-line B, which is the detector with cadmium, Similarly, the figure 3 represents the UV spectrum of Cu The maximum absorption peak appears at 579 nm, as mentioned in [23].with slight variation. where it is observed that the clear peak of copper disappears upon the addition of the toxic element Hg solution. As shown, curve A corresponds to Cu, while the straight-line B is the reagent with the mercury solution. X-ray diffraction technology is one of the most important techniques in determining the crystalline structure of a material [24]. (Figure 4 A) shows X-ray diffraction was used to determine the crystalline structure of the prepared copper nanoparticles, and the measurement showed the presence of pure copper, known for its face-centered cubic FCC crystalline structure. The results in Figure showed clear peaks at the angles (2Theta = 43.5°, 50.8°, 74.3°), which correspond to the crystal planes (111, 200, 220) according to the reference data JCPDS No. 04-0836 [25] also (figure 4 B) represent the X-ray diffraction patterns used to determine the crystal structure of nanostructured zinc oxide. The diffraction patterns were recorded in the angular range of (20 to 80 °) , The results showed conformity with the standards of hexagonal wurtzite zinc oxide, which corresponds to the International Card (JCPDS No 00-036-1451).The main crystalline levels were identified (2Theta =31.74°, 34.62°,36.34°, 47.64°, 56.9°, 62.9°, 67.86°)corresponding to the levels (111), (002), (101), (102), (110), (103), (112) respectively [26].

To determine the nanoscale dimensions of particles used (FESEM) and used (EDX) To measure the purity of the material, (figure 5 A,B) represents an FESEM image showing Cu NPs particles prepared in a spherical shape with some agglomeration, which enhances interactions with other materials [27]. It is also clear from the figure that the particles are approximately spherical in shape with an average size of D=72.71nm, where the dimensions were measured at a magnification of 200 nm. Moreover, (figure5 C) represents

EDX spectrum of Cu NPs, and the results show that the percentages of Cu 85.02%and O 14.98% are present, with no visible impurities, indicating the very high purity of the sample prepared by the green method this result matches previous studies [28], Likewise Through the FESEM analysis of the nanostructured zinc oxide and presenting the results as shown in(figure 6 A, B) nearly spherical particles were observed with an average size of D=28.29 nm. This result is very close to the previous study [29] and (The figure 6C) shows the EDX spectrum of ZnO NPs, and it is observed that there is a very high percentage of zinc and a peak for oxygen, indicating the formation of ZnO NPs Very small percentages of Na and N are also observed.

The TEM device was used to obtain clear images of particle sizes and shapes, (figure 7A) shows the TEM measurement of Cu NPs. The high precision indicates the crystalline nature of the model. Through the random field of the TEM image, the average diameter of Cu NPs was calculated by taking approximately 40 particles and measuring their diameters using the ImageJ program. The distribution shown in (figure 7 B), which represents particle size distribution within the range (5-27) nm and the majority are concentrated at (14-18) nm, (figure 8 A) represents the TEM microscopic analysis of zinc oxide nanoparticles, where they appear as homogeneous spherical aggregates. After selecting a specific area consisting of approximately 40 particles and using the ImageJ program to calculate the size, it was found that the sizes of the zinc oxide nanoparticles fall within the range of (31-87) nm, with the majority concentrated around the size of (45-52) nm, as shown in (figure 8B). The dynamic light scattering (DLS) technique is used to check the size and measure the zeta potential of the prepared nanoparticles, (figure 9A) shows zeta potential value for Cu NPs measured at an electrode Voltage of 3.9 V, which was found to be -27.0 mV. The negative charge indicates that the manufactured particles possess electrostatic repulsion and thus have good stability. Consequently, the high negative zeta potential leads to strong repulsion between the particles, causing an amplification or enhancement of their stability[30].The hydrodynamic size is pl=4842.4, as shown in(figure 9B), Also(The figure 10A) shows the zeta potential measurement of Zinc Oxide nanoparticles, where the potential peak of -22.3 mV indicates that the dispersed Zn O NPs are oriented with negative groups, proving their stability [31] and dynamic light scattering (DLS) technology to verify the hydrodynamic size, and thus the apparent PI value in (figure 10 B) for Zn O nanoparticle 1.643 . For the purpose of identifying functional groups FTIR was used. It is observed from the results obtained for measuring the infrared spectrum of the nanomaterials prepared by the green method that there are common or similar vibration peaks, which confirms the effectiveness of the plant extracts used ,(The figure11) represents the FTIR spectrum of Cu NPs, The peaks at 587.96 cm^{-1} and 690.67 cm^{-1} often represent the Cu-O vibration, which is the metal with oxygen, while the peaks at 479.19 cm^{-1} and 422.69 cm^{-1} represent the Cu vibration and 1446.61 cm^{-1} represent O-H stretching vibrations indicating the presence of hydroxyl groups[32], 1601.40 cm^{-1} represent N-H represent (amines, amides) bonds from plant extract,[33] however(figure12) represents the FTIR spectrum of Zn O NPs prepared by green synthesis. The biomolecules present in the plant extracts are responsible for reducing the nanoparticles, which show metal oxide absorption in the region below 1000 cm^{-1} with peaks at 531.21 cm^{-1}, 628.07 cm^{-1} and 661.44 cm^{-1} corresponding to zinc oxide nanoparticles, 1600.22 cm^{-1} represent suggesting the presence of sugars or carbohydrate compounds in the plant extract (aldehyde groups) [34], 3473.81 cm^{-1} represent O-H stretching vibrations indicating the presence of hydroxyl groups[32].

Factors effecting the sensing process

The effect time on the detection of mercury and cadmium

The effect of time on the detection of mercury and cadmium ions was studied starting from the moment the sample was added until 5 minutes had passed. A noticeable color change was observed during the first few seconds, indicating a rapid initial reaction between the surface of the detector and the ions. The change continued to increase gradually until it stabilized after approximately 5 minutes (Figure 13). Based on this, 5 minutes is considered the ideal time to achieve maximum detection efficiency under the experimental conditions used.

Effect of Interfering Ions on the Detection of Hg^{+2} and Cd^{2+}

The effect of the interferences was evaluated to verify the selectivity of the detector by studying the impact of the presence of other metal ions such as Ca^{2+}, Mg^{2+}, PO_4^{3-}, K^+, Na^+, SO_4^{2-}, CO_3^{2-}, Cl^-, and NO_3^-, as well as nitrogenous compounds like urea, creatinine, and uric acid at concentrations comparable to or higher than the target ion (Hg^{+2} and Cd^{2+}) concentration. The results showed that these ions did not significantly affect the detection signal, indicating high selectivity of the system.

Performance of Nano sensors

The detection of Havey metal (mercury and cadmium) in blood

The calibration curve was plotted in (figure 14) using the absorbance measured at five concentrations (0.5, 1 ,1.5 ,2 ,2.5) mg/L. To illustrate the relationship between the concentration of heavy metals (Hg^{+2} and Cd^{+2}) and absorbance. The results showed two linear curves represented by two equations, where the correlation coefficient reached (0.221), indicating a satisfactory linear relationship between the concentration of Hg^{+2} and absorption. Similarly, the R^2 for Cd^{+2} indicated (0.26) an excellent fit with the linear model.

The microfluidic device printed using 3D printing technology with a dual design for the simultaneous detection of heavy metals (Hg, Cd) in blood plasma samples, as shown in (Figure 14), consists of a main channel in the center dedicated to blood plasma, from which two arms extend dedicated to sensors (Cu NPs, ZnO NPs). After injecting the plasma into the central channel in a specific amount and adding the substances to be detected, and when they reach the sensors injected in the specified channels, the resulting color is captured using an iPhone 12 Pro Max and a regular camera. After processing the data, quantitative measurement is performed using the ImageJ software. (Figure 14) illustrates the detection steps.

Conclusion

In this study, copper and zinc oxide nanoparticles were prepared using frankincense extract. For the purpose of characterizing the prepared particles, diagnostic measurements (UV, XRD, FESEM, TEM, FT-IR and ZETA POTANTIOAL) were conducted. The prepared materials were used to detect heavy metals in blood plasma, where zinc oxide acted as a detector for cadmium ions at the lowest concentration and copper detected mercury ions at the lowest concentration that could be present in blood plasma. The detection was achieved through a color change when the reagent was added to the substance being detected. To increase the accuracy and speed of detection, we designed a small microfluidic device with fine capillary channels, where these channels, in conjunction with the nanoparticles, enhance the speed and accuracy of detection.

1.3. Figures

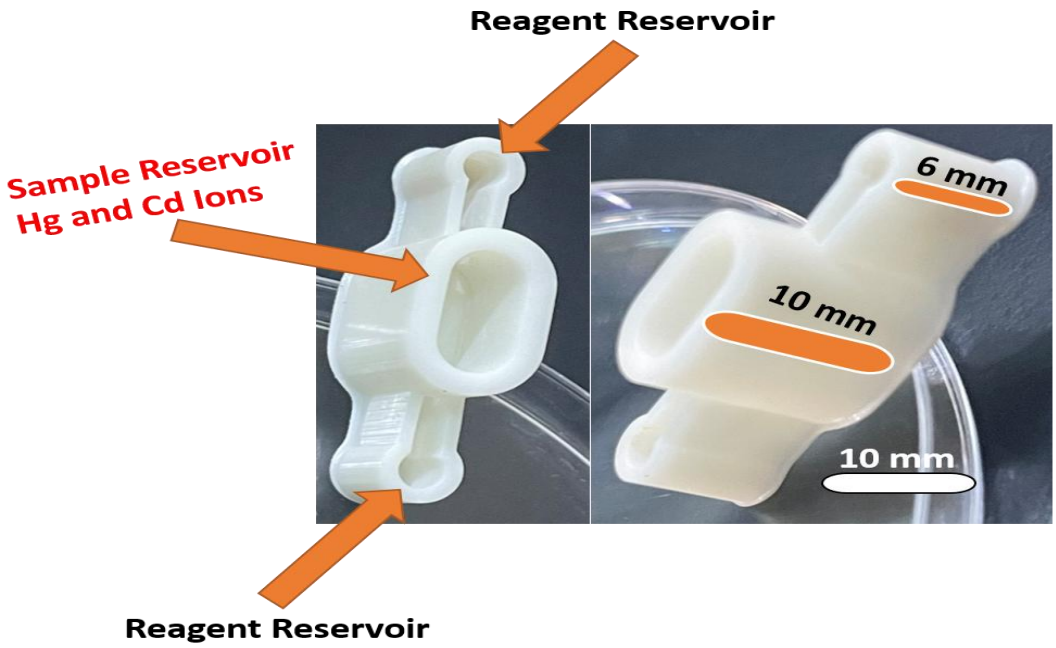

Figure. 1. Photograph image of the 3D printed microfluidic device for dual device with a main channel in the center and two channels. The image with Scale bar 10mm.

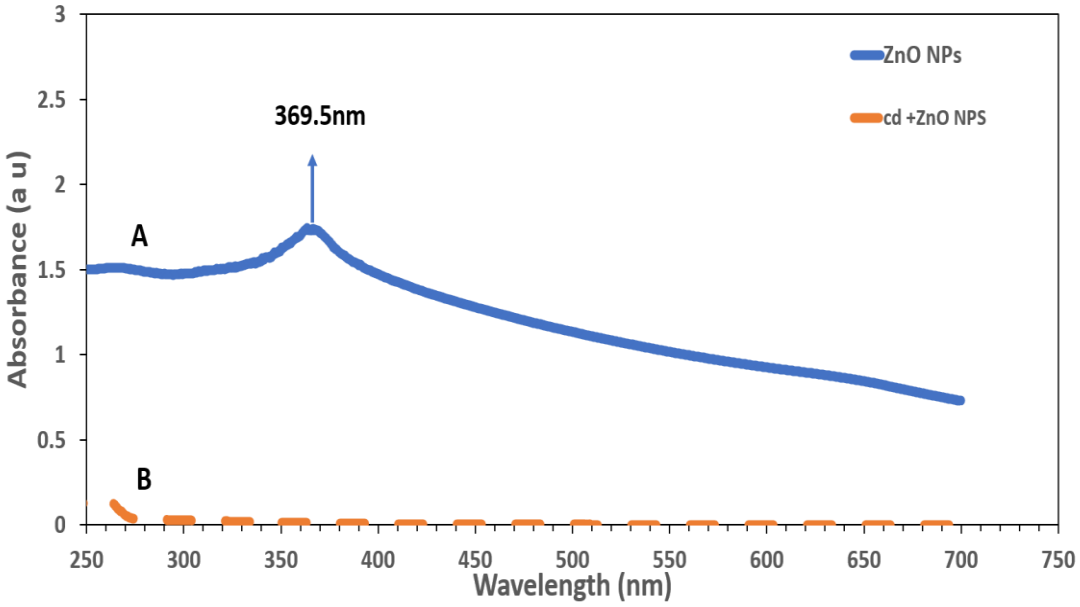

Figure. 2. UV-Visible spectra of A (blue line) ZnO nanoparticles, B (orange line) absorption spectrum after adding ZnO to the cadmium solution.

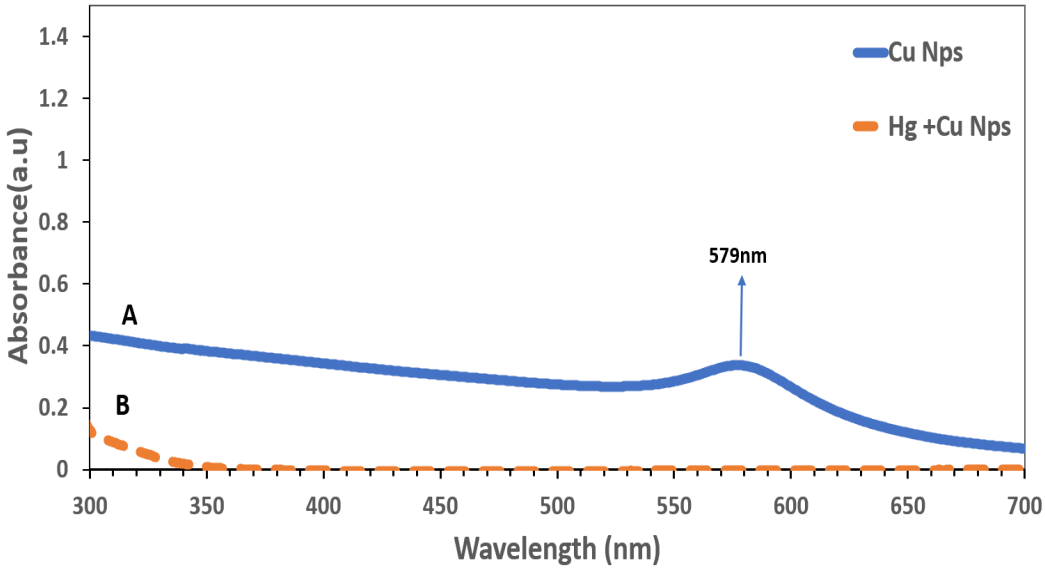

Figure. 3. UV-Visible spectra of A (blue line) Cu nanoparticles, B (orange line) absorption spectrum after adding Cu NPs to the mercury solution.

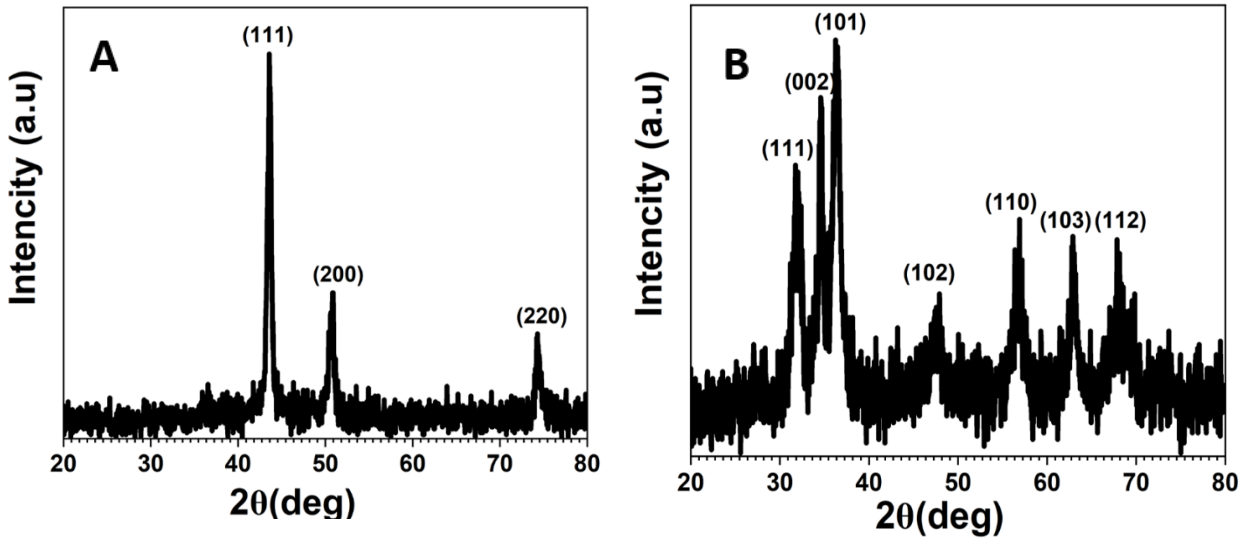

Figure. 4. XRD powder pattern of the crystalline (A) ZnO NPs (B) Cu NPs.

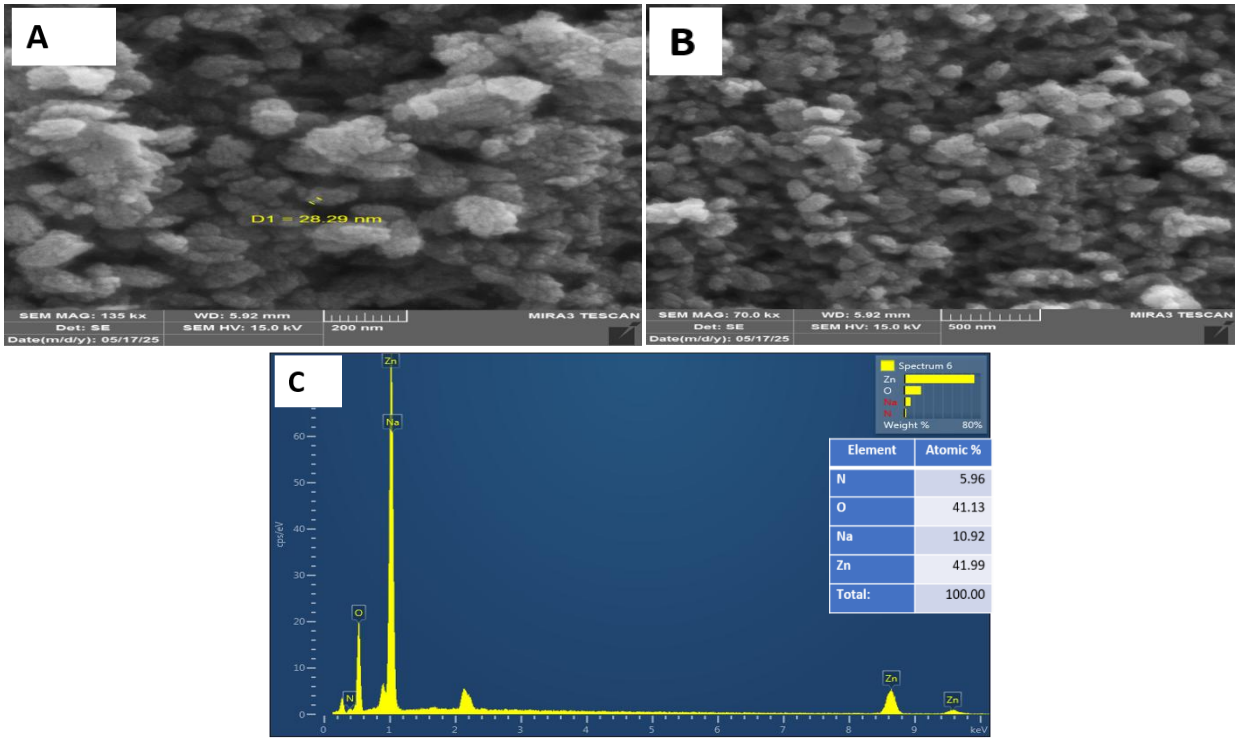

Figure. 5. FESEM images of the green-synthesized of zinc oxide nanoparticles (A) At 200 nm and (B) At 500 nm

(C) EDX spectroscopy of zinc oxide nanoparticles.

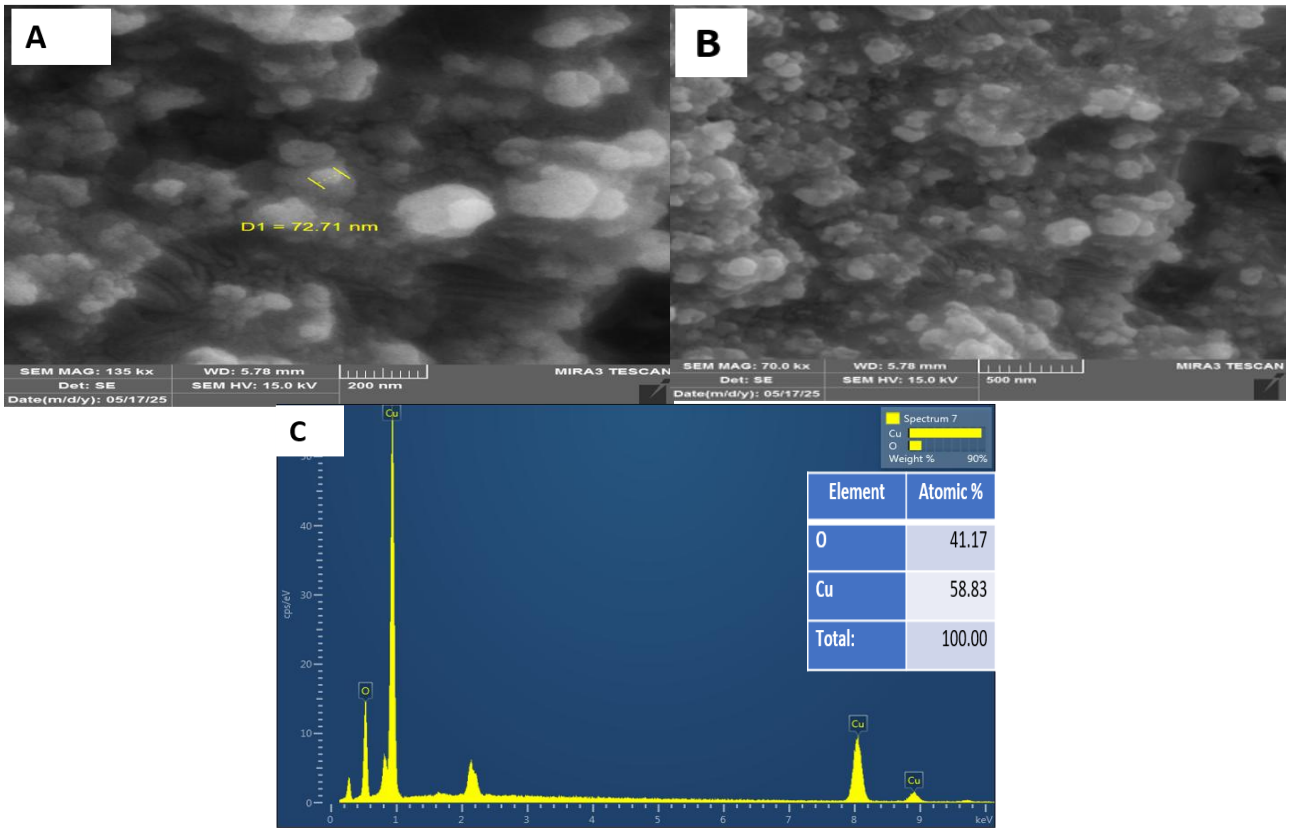

Figure. 6. FESEM images of the green-synthesized of copper nanoparticles (A) At 200 nm and (B) At 500 nm (C) EDX spectroscopy of copper nanoparticles.

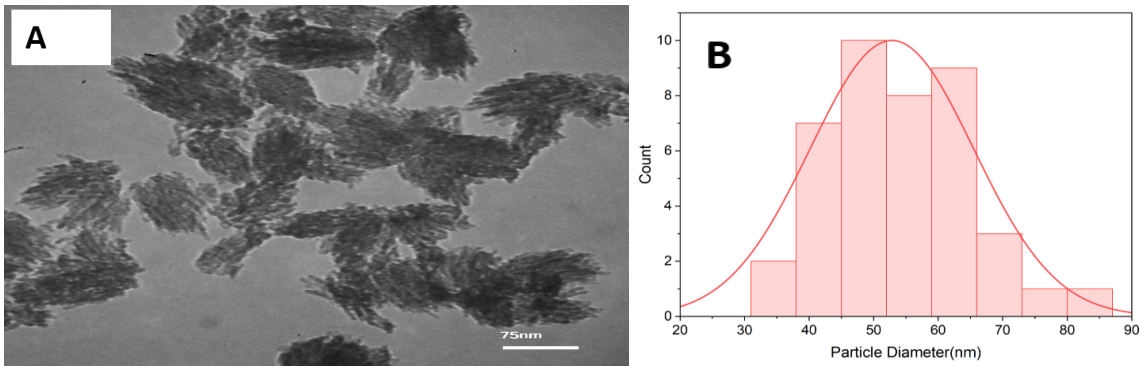

Figure .7. TEM measurement of the green-synthesized ZnO NPs nanoparticles(A), and size distribution(B).

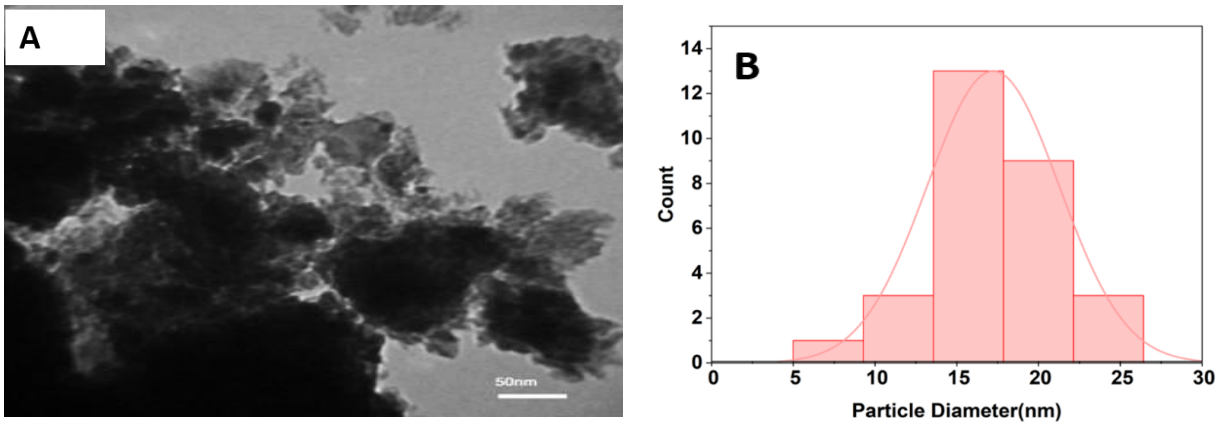

Figure .8. TEM measurement of the green-synthesized Copper nanoparticles (A), and size distribution(B).

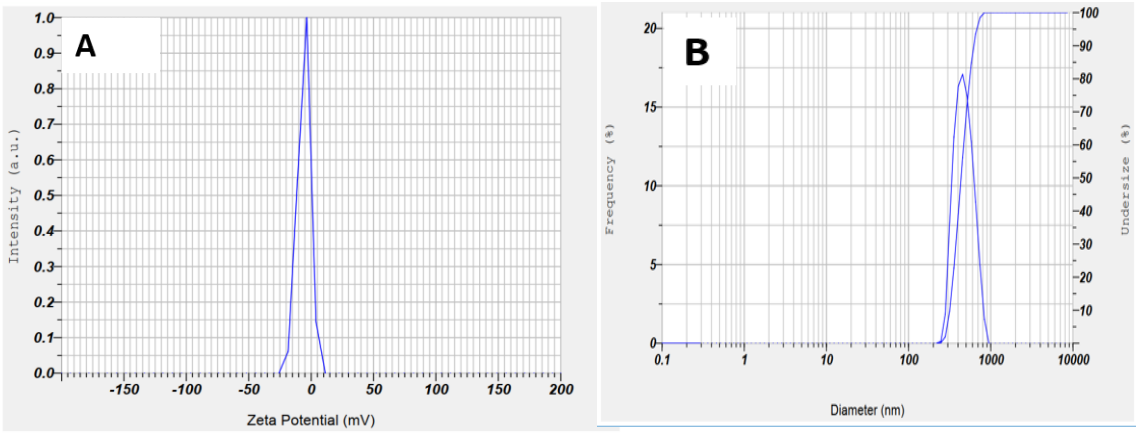

Figure . 9. (A) zeta potential analysis of Zinc Oxide nanoparticles (B) dynamic light scattering of Zinc Oxide nanoparticles.

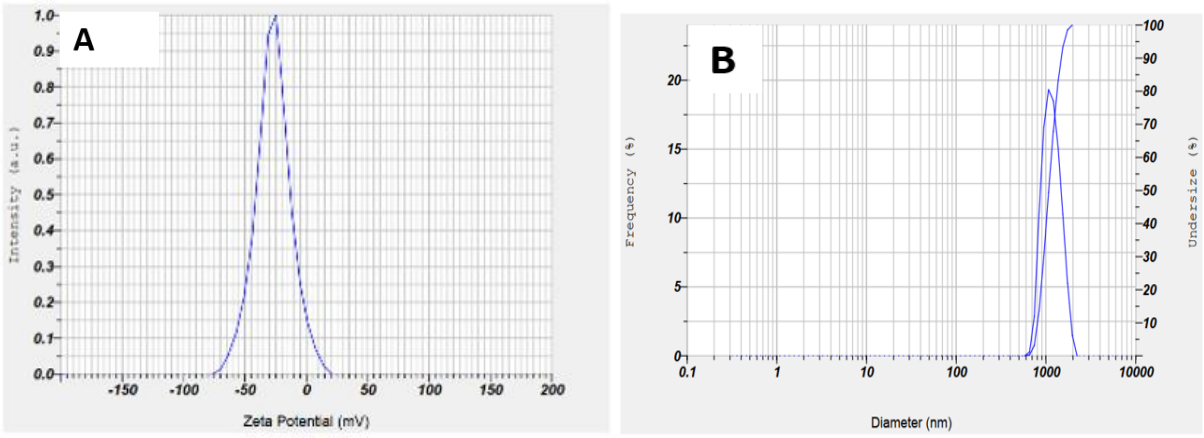

Figure .10. (A) zeta potential analysis of copper nanoparticles (B) dynamic light scattering of s Copper nanoparticles.

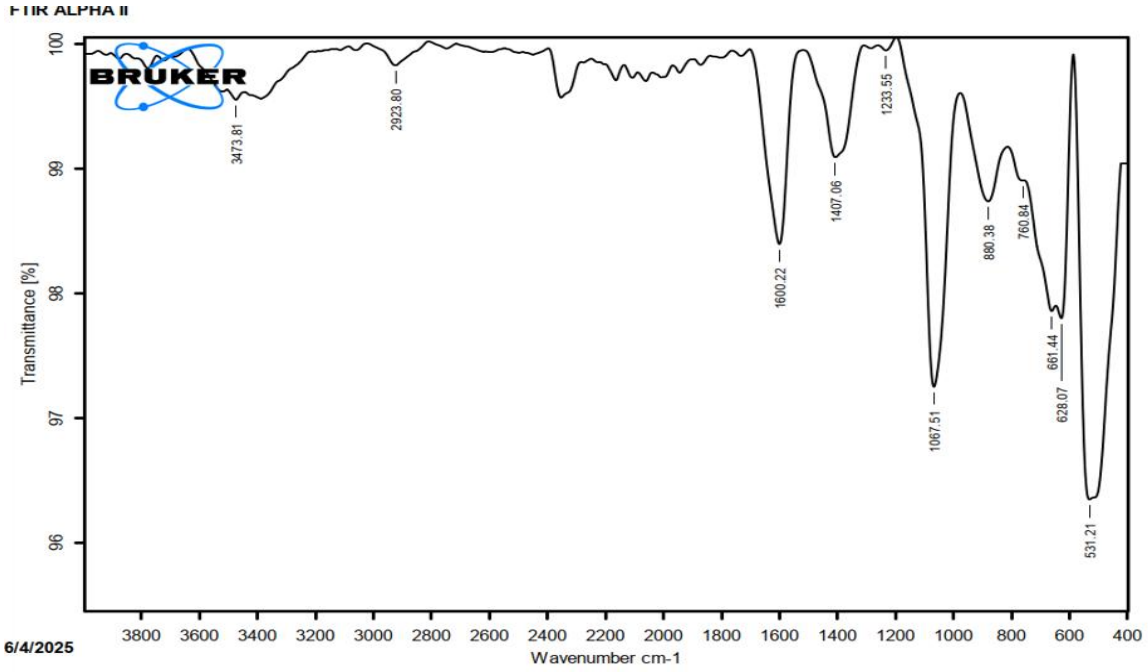

Figure. 11. FTIR spectrum of ZnO Prepared by Boswell sacra.

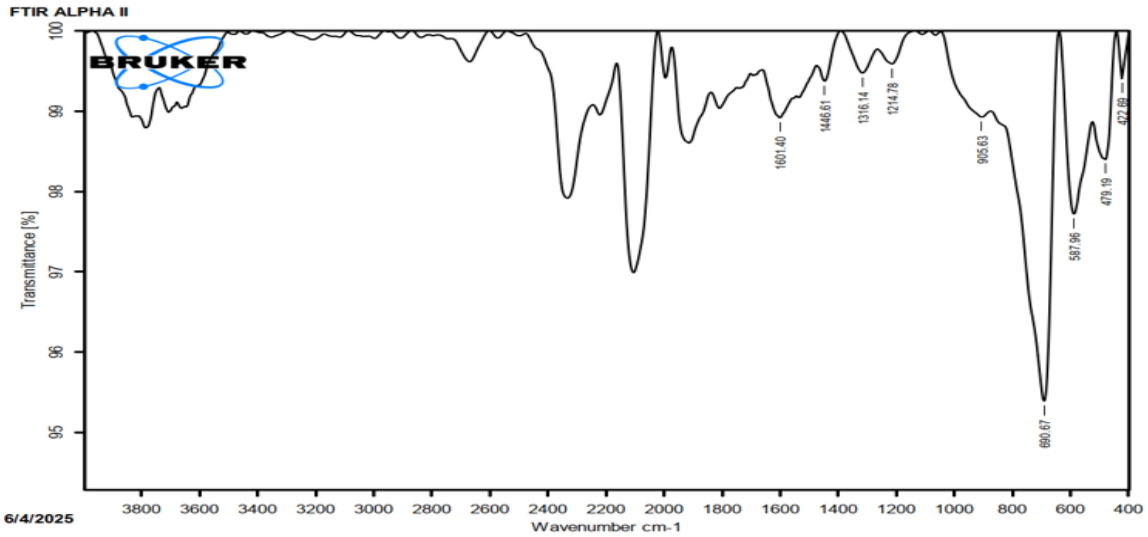

Figure .12. FTIR spectrum of Cu NPs prepared by Boswell sacra.

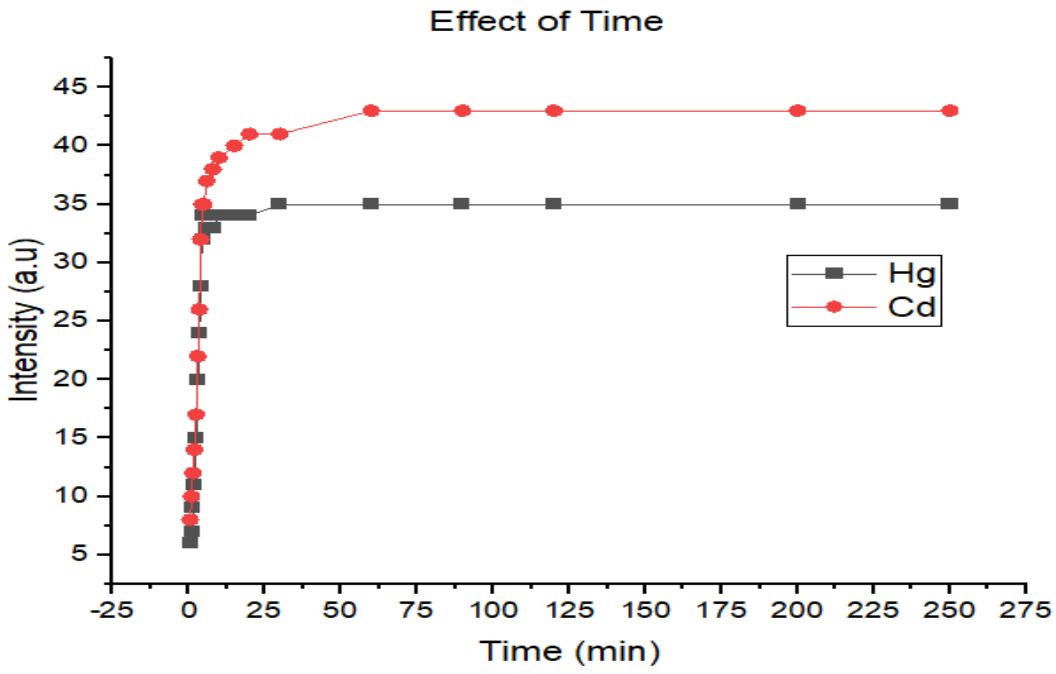

Figure 13: Effect of time on the detection of mercury and cadmium by ZnO NPs and Cu NPs.

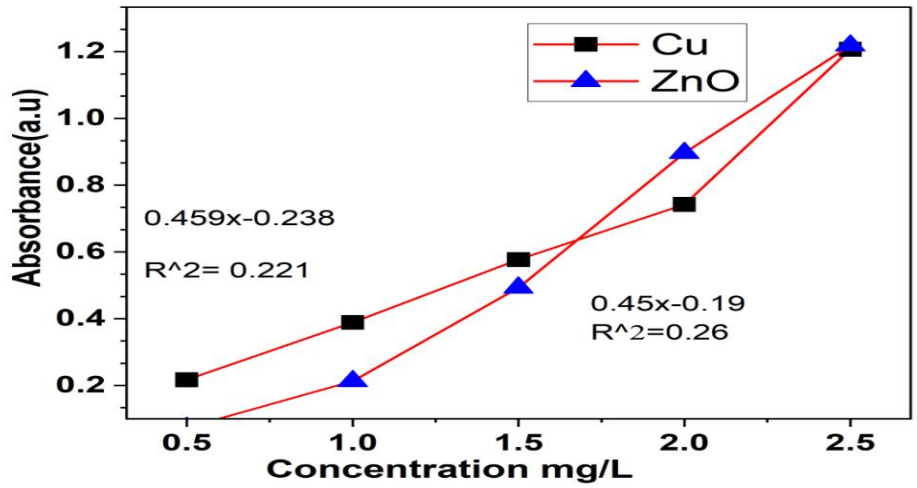

Figure. 14. The calibration curve for detecting Hg^{+2} by Cu NPs and Cd^{+2} by ZnO NPs, Figure illustrates the relationship between intensity and element concentration.

Acknowledgments

Acknowledgments must be unnumbered. These should be kept to a minimum. Authors should list all funding sources in the Acknowledgments section. Authors are responsible for the accuracy of their funder designation.

REFERENCES

[1] Balali-Mood, M., et al., *Toxic mechanisms of five heavy metals: mercury, lead,*

chromium, cadmium, and arsenic. Frontiers in pharmacology, 2021. **12**: p. 643972.

[2] Al-Aqbi, Z.T., Yap, Y.C., Li, F. and Breadmore, M.C. Integrated microfluidic devices fabricated in poly (methyl methacrylate) (PMMA) for on-site therapeutic drug monitoring of aminoglycosides in whole blood. Biosensors, 2019. 9(1): p.19[3] Viegas, S., C. Martins, and R. Assunção, Human biomonitoring (HBM) as a tool to support policy and regulatory action to prevent chemicals exposure. 2024, Frontiers Media SA. p. 1376890.

[4] Ma, L., et al., *A new thiacalix [4] arene-based metal-organic framework as an efficient electrochemical sensor for trace detection of Cd2+ and Pb2+.* Food Chemistry, 2024. **441**: p. 138352.

[5] Wang, Y., et al., *Detection of Ultra-Trace Heavy metals in Aerosols with pg^ m3 Sensitivity Using Filament-Induced Fluorescence Spectroscopy.* arXiv preprint arXiv:2506.09295, 2025.

[6] Andoh, P.K.D., *Development of Novel Electrochemical Sensor to Detect Heavy Metals Cadmium, Lead and Chromium*. 2025, Wright State University.

[7] Fakayode, S.O., et al., *Electrochemical and colorimetric nanosensors for detection of heavy metal ions: a review.* Sensors, 2023. **23**(22): p. 9080.

[8] Rai, M., A. Yadav, and A. Gade, Silver nanoparticles as a new generation of antimicrobials. Biotechnology advances, 2009. 27(1): p. 76-83.

[9] Wang, H., et al., Preparation of silver nanoparticles by chemical reduction method. Colloids and Surfaces A: Physicochemical and Engineering Aspects, 2005. 256(23):p. 111-115.

[10] Pricop, A., et al., *Copper Nanoparticles Synthesized by Chemical Reduction with Medical Applications.* International Journal of Molecular Sciences, 2025. **26**(4): p. 1628.

[11] Logutenko, O., et al., *A novel method to prepare copper microspheres via chemical reduction route.* Journal of Materials Research and Technology, 2021. **13**: p. 1254-1265.

[12] Anjum, S., et al., *Recent advances in zinc oxide nanoparticles (ZnO NPs) for cancer diagnosis, target drug delivery, and treatment.* Cancers, 2021. **13**(18): p. 4570.

[13] Moussa, N., et al., *Chromium doped ZnO nanoparticles for energy storage, gas and humidity sensing and spin based electronic devices applications.* Optical and Quantum Electronics, 2022. **54**(11): p. 683.

[14] Hegde, V.N., *Study on structural, morphological, elastic and electrical properties of ZnO nanoparticles for electronic device applications.* Journal of Science: Advanced Materials and Devices, 2024. **9**(3): p. 100733

.

[15] Han, X., et al., Polymer-based microfluidic devices: a comprehensive review on preparation and applications. Polymer Engineering & Science, 2022. 62(1): p. 3-24.

[16] Nie, C., I. Shaw, and C. Chen, Application of microfluidic technology based on surface-enhanced Raman scattering in cancer biomarker detection: A review. Journal of Pharmaceutical Analysis, 2023. 13(12): p. 1429-1451.

[17] Liu, W., H. Cheng, and X. Wang, Skin-interfaced colorimetric microfluidic devices for on-demand sweat analysis. npj Flexible Electronics, 2023. 7(1): p. 43.

[18] Al-aqbi, Z.T., Abdulsahib, H.T. and Al-Doghachi, F.A.. A Portable Microfluidic Device-Based Colorimetric Naked-Eye Sensors for Determination ofMercury and Arsenic Ions in River Water Samples. Plasmonics, 2024. pp.1-22.

[19] Charkiewicz, A.E., et al., *Cadmium toxicity and health effects—a brief* summary. Molecules, 2023. **28**(18): p. 6620.

[20] AL-AQBI, Z.T., ALBISHRI, A., HUSSEIN, F.H., ALBUKHATY, S., SULAIMAN, G.M., KHALIL, K.A. and AHMED, E.M. A new 3D printing milli-fluidic device with integrated nanojunction for on-site colorimetric analysis of iron in water and soil samples. Chinese Journal of AnalyticalChemistry, 2025. 53(1), p.100475.

[21] Shahwan, T., et al., Green synthesis of iron nanoparticles and their application as a Fenton-like catalyst for the degradation of aqueous cationic and anionic dyes. Chemical Engineering Journal, 2011. 172(1): p. 258-266.

[22] Mojgan Ebadi, a.M.R.Z., a Seyyed Soheil Aghaei,a Mohsen Zargar,a and b.H.S.Z.a.K.A.N. Morvarid Shafiei, *A bio-inspired strategy for the synthesis of zincoxide nanoparticles (ZnO NPs) using the cell extractocyanobacterium Nostoc sp. EA03: from*

[23] Ani Qomariyah*, A.K.H., *Synthesis of Copper Nanoparticles Using Dragon Fruit (Hylocereus polyrhizus) Extract as a Bio*

[24] Sadia, B.O., J.K. Cherutoi, and C.M. Achisa, *Optimization, characterization, and antibacterial activity of copper nanoparticles synthesized using senna didymobotrya root extract.* Journal of Nanotechnology, 2021. **2021**(1): p. 5611434.

[25] Ambati, T., et al., *Efficacy of copper oxide nanoparticles using Piper longum and Piper betle.* Bioinformation, 2023. **19**(9): p. 964.

[26] Almoneef, M.M., et al., *Exploring the multi-faceted potential: Synthesized ZnO nanostructure–Characterization, photocatalysis, and crucial biomedical applications.* Heliyon, 2024. **10**(12)

[27] Ibrahim, F.M., D.A. Najeeb, and H. ThamerSadeq, *Green preparation of Cu nanoparticles of the avocado seed extract as an adsorbent surface.* Materials Science for Energy Technologies, 2023. **6**: p. 130-136.

[28] Godse, J.S., et al., *Synthesis Characterization and Antimicrobial Activity of Copper Oxide Nanoparticles Using Sol-Gel Method.* Clinical Interventions and Clinical Trials, BRS Publishers, 2023. **1**(1): p. 2993-1096.

[29] Roy, S., R. Priyadarshi, and J.-W. Rhim, *Development of multifunctional pullulan/chitosan-based composite films reinforced with ZnO nanoparticles and propolis for meat packaging applications.* Foods, 2021. **10**(11): p. 2789.

[30] Sadia, B.O., J.K. Cherutoi, and C.M. Achisa, *Optimization, characterization, and antibacterial activity of copper nanoparticles synthesized using senna didymobotrya root extract.* Journal of Nanotechnology, 2021. **2021**(1): p. 5611434.

[31] Khan, M., P. Ware, and N. Shimpi, *Synthesis of ZnO nanoparticles using peels of Passiflora foetida and study of its activity as an efficient catalyst for the degradation of hazardous organic dye.* SN Applied Sciences, 2021. **3**: p. 1-17.

[32] Vijaya Kumar, P., A. Jafar Ahamed, and M. Karthikeyan, *Synthesis and characterization of NiO nanoparticles by chemical as well as green routes and their comparisons with respect to cytotoxic effect and toxicity studies in microbial and MCF-7 cancer cell models.* SN AppliedSciences, 2019. **1**: p. 1-15.

[33] Pasieczna-Patkowska, S., M. Cichy, and J. Flieger, *Application of Fourier transform infrared (FTIR) spectroscopy in characterization of green synthesized nanoparticles.* Molecules, 2025. **30**(3): p. 684.

[34] Thangeeswari, T., A.T. George, and A.A. Kumar, *Optical properties and FTIR studies of cobalt doped ZnO nanoparticles by simple solution method.* Indian J. Sci. Technol, 2016. **9**(1): p. 1-4.